Self-seeding synthesis of silver nanosheets with binary reduction in poly (vinylpyrrolidone)–sodium dodecyl sulphate aggregation microreactor

Ye Fan[1], *Yueping Ren*[1,2], *Yun Fang*[1], *Menjie Wu*[1]

[1]*The Key Laboratory of Food Colloids and Biotechnology, Ministry of Education, School of Chemical and Material Engineering, Jiangnan University, Wuxi, Jiangsu 214122, People's Republic of China*
[2]*School of Environmental and Civil Engineering, Jiangnan University, Wuxi, Jiangsu 214122, People's Republic of China*
E-mail: yunfang@126.com

Published in Micro & Nano Letters; Received on 10th February 2014; Revised on 17th August 2014; Accepted on 9th September 2014

Silver (Ag) nanosheets were synthesised through a facile self-seeding strategy with binary reduction in the poly(vinylpyrrolidone) (PVP)–sodium dodecyl sulphate (SDS) aggregation microreactor, in which the size and morphology of Ag nanoparticles were able to be regulated by concentration or pH dependence. In this approach, PVP and SDS built the microreactor together and served as a synthesis template; a trace of sodium borohydride ($NaBH_4$) was employed to rapidly trigger the competitive formation of small Ag seeds, while PVP was responsible for the subsequent reduction and slow crystal growth. The size and morphology of the nanosheets could be gently regulated with the concentrations of PVP or SDS and the pH of the reaction solution; while the dramatic variance of size and morphology was primarily induced by $NaBH_4$ concentration. Free PVP monomers with lower concentration induced irregular particles, while the lower concentration of $NaBH_4$ led to the formation of small and regular nanosheets. Both particle size and morphology could be regulated with SDS concentration dependence if the SDS concentration was higher than the critical aggregation concentration. Higher SDS concentrations favoured smaller particle sizes and nanosheet formation. Two-dimensional planar Ag nanostructures were generated at pH 9–10, where $[Ag(NH_3)_2]^+$ existed at a stable complex ionisation state.

1. Introduction: Anisotropic silver (Ag) nanostructures have received wide and intensive interest [1–11]. In recent years, various synthetic approaches have been applied in the controlled fabrication or morphology modulation of Ag nanostructures, including hydrothermal [12], $NaBH_4$ reduction using citrate and poly(vinylpyrrolidone) (PVP) as stabilisers [1], polyol reduction [13] or UV [2, 14]/microwave radiation [15] reduction, electrochemical deposition [16], microemulsion [17] and vapour deposition [18]. However, the preparation strategies for two-dimensional (2D) Ag nanostructures were relatively limited. As was reported, 2D Ag nanostructures were usually prepared through seed-mediated synthesis in organic solvents with thermal or UV assistance [19–25]. Ag nanoplates were obtained by using ultrasonic-assisted Ostwald ripening in *N*, *N*-dimethylformamide in the presence of PVP [24]. Sarkar *et al.* [20] adopted a seed-mediated route to synthesise Ag nanodiscs, utilising hydroxypropyl methyl cellulose as a stabilising agent and extra small nanoparticles as seeds in an aqueous solution. They found that additional citrate ions play the pivotal role in controlling the size of Ag nanodiscs. Nevertheless, most of these reported synthetic strategies needed additional seeds, long ripening processes or organic solvents. A one-step and cost-effective synthesis of Ag nanosheets by the oil/water interfacial method was developed [26], but benzene was also needed to construct the oil/water interface and the products were in micrometre scale. So more facile and environment benign approaches for the synthesis of 2D Ag nanostructures are still urgently needed.

Polymer–surfactant aggregations were better templates for synthesising nanostructures than the surfactant or polymer used alone [27, 28]. PVP was used as a weak reductant and stabiliser in the synthesis of noble metal nanostructures [29, 30], while PVP–sodium dodecyl sulphate (SDS) aggregations provided a nice template to obtain gold nanoflowers [29] and multipod-like gold nanoparticles [31] in aqueous solutions. In addition to PVP, sodium borohydride ($NaBH_4$) was recognised as a very popular and strong reductant used in the synthesis of noble metal nanostructures.

In tentative experiments, we found that $NaBH_4$ mainly induced the formation of small Ag nanoparticles just like most researchers reported, while PVP alone led to the generation of irregular Ag nanostructures. Truncated triangular Ag nanoplates could only be fabricated when a trace of $NaBH_4$ and a large amount of PVP were used simultaneously in this experiment, while novel hollow Ag spheres have been reported by other researchers when using $NaBH_4$ and PVP simultaneously [11]. Therefore, a syn of these two reductants in this Letter was expected to obtain different 2D Ag nanostructures by manipulating their concentration or environment factors, such as pH and each component concentration in the PVP–SDS aggregations. Therefore, in this experiment, Ag nanosheets were fabricated by self-seeding through a facile binary reductant strategy run in the aqueous solution of PVP–SDS aggregations. The trace of $NaBH_4$ was introduced in the early phase to generate tiny Ag nanocrystals that were used as the seeds for the subsequent growth of Ag nanoplates, in which PVP served as a mild reducing agent and as the supplement of $NaBH_4$. In this synthesis process, PVP–SDS aggregations virtually acted as microreactors which controlled the formation of Ag nanoplates through two assembling processes. In the first assembly, the sizes of primary Ag nanocrystals were mainly affected by the template effect of SDS bound micelles. Subsequently, PVP selectively absorbed on certain crystal planes exerted a reducing effect to modulate the asymmetrical growth of Ag nanocrystals. This approach can coordinate Ag crystal growth characteristics with the modulating effect of PVP–SDS microreactors, and expand applications of this sort of microreactors in the preparation of metal micro/nanostructures.

2. Experimental

2.1. Materials: $AgNO_3$ (Sinopharm Chemical Reagent Co. Ltd, analytical reagent grade), PVP (International Specialty Products, Inc., chemical reagent grade), SDS (Acros Organics Co. Ltd, 99%), $NaBH_4$ (Sinopharm Chemical Reagent Co. Ltd, analytical reagent grade) and $NH_3{\cdot}H_2O$ (Sinopharm Chemical Reagent Co. Ltd, analytical reagent grade) were used without further

doi: 10.1049/mnl.2014.0076

purification. Ultrapure Millipore water (18.2 MΩ·cm) was used throughout.

2.2. Self-seeding preparation of Ag nanosheets using binary reductants in the microreactor of PVP–SDS aggregations: $AgNO_3$ and $NH_3{\cdot}H_2O$ were mixed with the molar ratio of 1:2 to prepare the Ag–NH_3 complex solution (5 mM). In a typical synthesis, a certain amount of Ag–NH_3 complex solution, PVP solution, SDS solution and ultrapure water were added to a 10 ml vial in sequence. After homogeneous mixing, the 10 ml vial was immersed into a water bath at 40°C for 1 h. $NaBH_4$ (1 mM) was then quickly added to a 10 ml vial which was then stored in a 40°C water bath and kept in the dark for another 7 h.

2.3. Characterisation: The X-ray diffraction (XRD) pattern was recorded using a Bruker D8 advance X-ray diffractometer equipped with graphite-monochromated Cu Kα radiation. The UV–vis spectra were recorded by Persee T6 UV–vis spectroscopy. Transmission electron microscope (TEM) images and the high-resolution transmission electron microscope (HRTEM) image were obtained on a JEOL JEM-2100 TEM operated at an accelerating voltage of 200 kV. Surface tensions (γ) of PVP (15 g/L)–$[Ag(NH_3)_2]^+$ (1 mM)–SDS ternary aqueous solutions with varying SDS concentrations were measured with the Wilhelmy method at 25°C using the surface tension instrument DCA 315 (Thermo Cahn).

3. Results and discussion

3.1. Morphology of Ag nanosheets generated by self-seeding preparation: As aforementioned, truncated triangular Ag nanosheets could only be fabricated when a trace of $NaBH_4$ and a large amount of PVP were used simultaneously. Hence, in the presence of PVP–SDS, $[Ag(NH_3)_2]^+$ was reduced to Ag nanosheets with a trace of $NaBH_4$ as shown in Fig. 1.

Time-dependent UV–vis spectra of the reaction mixture (Fig. 1*a*) indicates the reduction procedure of $[Ag(NH_3)_2]^+$. A weak plasmon resonance peak at 450 nm immediately appears upon the addition of $NaBH_4$, which can be attributed to the incipient formation of Ag nanocrystals. An apparent red shifting of the plasmon resonance occurs during the reaction. At 7 h, the products exhibit a strong plasmon resonance peak at about 540 nm which normally appears as in-plane dipole plasmon resonance of planar Ag nanostructures [32]. The XRD pattern (Fig. 1*b*) reflects that the as-synthesised Ag nanostructures are in the face-centred-cubic (fcc) phase. Five peaks observed in the 2θ range of 30°–85° can be indexed to the (111), (200), (220), (311) and (222) reflections, respectively. The TEM image (Fig. 1*c*) reveals that the obtained Ag nanostructures are truncated nanosheets with 70 nm in edge length. The fringe spacing measured from the HRTEM image (Fig. 1*d*) is 0.236 nm, which is equated with the lattice spacing of Ag(111).

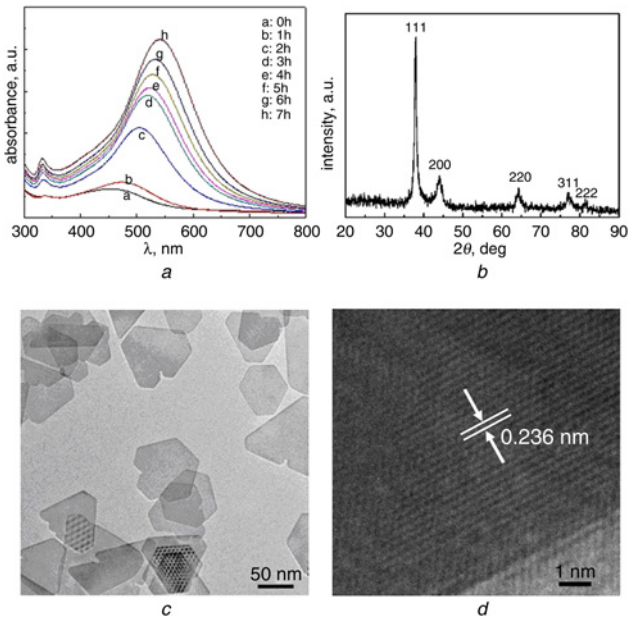

Figure 1 *UV–vis spectra (Fig. 1a), XRD pattern (Fig. 1b), and TEM image (Fig. 1c) and HRTEM image (Fig. 1d) of the Ag nanosheets*
PVP, 15 g/l; SDS, 15 mM; $[Ag(NH_3)_2]^+$, 1 mM; $NaBH_4$, 0.0005 mM
Growth time of the nanoparticles in (Figs. 1*b* and *c*) was 7 h

3.2. Microreactor of PVP–SDS aggregations for the self-seeding growth of nanosheets: PVP is a well-known non-ionic polymeric template for nanoparticle synthesis, and PVP–SDS can self-assemble into aggregations with significant surface ordering [33, 34], therefore it could serve as a template or microreactor to generate various morphologies of nanoparticles [29, 31, 35, 36]. SDS and PVP self-assemble into –3D necklace-like aggregations once the SDS concentration exceeds the critical aggregation concentration (cac) [37, 38], and the cac can be obtained from the γ-lgc_{SDS} curve of the PVP–SDS solutions (Fig. 2*a*). Fig. 2*a* indicates that an SDS concentration of 5.24 mM is a threshold in the presence of 15 g/l of PVP, SDS and PVP exist as free monomers separately below this threshold but assemble into aggregations above this threshold. The so-called PVP–SDS aggregations have a necklace-like structure as indicated in Fig. 2*b*, in which SDS bound micelles acting as the 'beads' are linked by PVP as the 'strings'. These necklace-like aggregations served as microreactors in the growth of Ag nanosheets. As suggested in Fig. 2*c*, $[Ag(NH_3)_2]^+$ ions in the reaction solution would be enriched around SDS micelles that bound on PVP chains through electrostatic interaction. Once a trace of $NaBH_4$ is added, it triggers rapid reduction of $[Ag(NH_3)_2]^+$ by virtue of its intensive reducing power and immediate generation of small Ag seeds. Subsequently, PVP becomes the sole reducing agent in the growth of Ag nanocrystals as the trace of $NaBH_4$ is consumed quickly. The surface free energies of low-index facets for Ag nanocrystals were reported to increase in the following order: $\gamma(111) < \gamma(100) < \gamma(110)$ [39]. As PVP can selectively bind to Ag (100) [40] and PVP chains are the sole reductants in the subsequent growing stage, thus $[Ag(NH_3)_2]^+$ ions are reduced by PVP near Ag(100). Therefore, the (100) facets remain towards the continuous addition of Ag atoms rather than (111) facets uncovered by PVP, and the growth on Ag(100) will be preferential. This asymmetrical growth results in the ultimate formation of a 2D planar morphology with (111) as the dominant

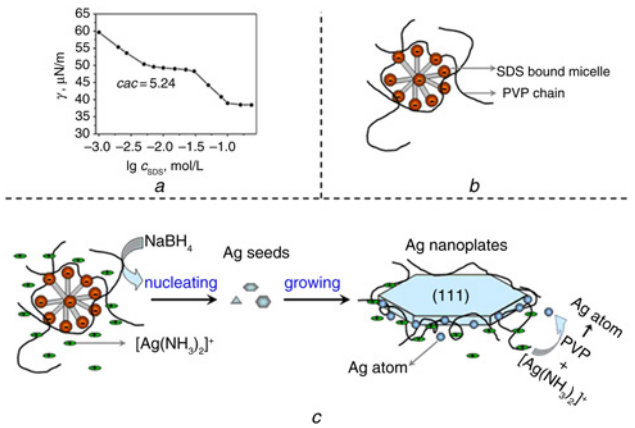

Figure 2 *γ-lgc_{SDS} curve of PVP (15 g/l)–SDS–$[Ag(NH_3)_2]^+$ (1 mM) aqueous solution (Fig. 2a); model of PVP–SDS aggregations (Fig. 2b); growth mechanism of Ag nanoplates (Fig. 2c)*

basal facet, which is consistent with the XRD pattern in Fig. 1*b*. These Ag atoms grow into anisotropic Ag nanosheets under the influence of PVP by selective adsorption onto different crystal facets to control the growing rates of them (Fig. 2*c*) [41].

3.3. Concentration dependence of the morphologies of Ag nanostructures: The concentration of the reductant would influence the reduction kinetics and decide the size and size distribution of the final reductive products, and in a similar way the concentrations of SDS and PVP would influence the size of the products since they affect the template formation as described in Fig. 2. Therefore, sizes of Ag nanoparticles depending on the concentrations of $NaBH_4$, PVP and SDS were investigated and the experimental results are shown in Figs. 3, 4 and 5, respectively. As was reported, there formed steady PVP–SDS aggregations when 15 g/l of PVP mixed with 15 mM or more of SDS [29].

As shown in Fig. 3, the concentration of $NaBH_4$, the primary reductant, induced a dramatic difference on both the size and the morphology of the particles. In the experiment, the addition of 0.0005 mM $NaBH_4$ turned the colour of the reaction solution instantaneously into light yellow, which indicated the appearance of small Ag particles. Subsequently, these Ag seeds grew into nanosheets slowly caused by the mild reduction of PVP as shown in Fig. 3*a*. Ag nanosheets were still the dominant morphologies at a higher concentration of reductant (Fig. 3*b*, 0.002 mM). However, multipod-like Ag nanoparticles appeared at 0.005 mM of $NaBH_4$ (Fig. 3*c*), which implied exorbitant Ag seeds trended to aggregates.

As for the role of PVP in the nanoparticle fabrication, it actually acted as not only one of the components of PVP–SDS aggregations but as a mild reducing agent. The PVP concentrations responded to the particle size once they fell in the assembly concentration range (Figs. 4*b* and *c*). PVP presented as free monomers with lower concentration and induced irregular particles (Fig. 4*a*).

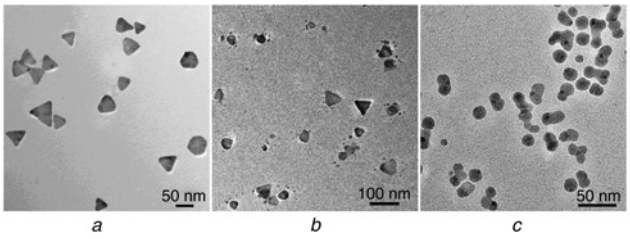

Figure 3 *TEM images of Ag nanostructures synthesised at different $NaBH_4$ concentrations*
a 0.0005 mM
b 0.002 mM
c 0.005 mM
PVP, 15 g/l; SDS, 15 mM; $[Ag(NH_3)_2]^+$, 1 mM

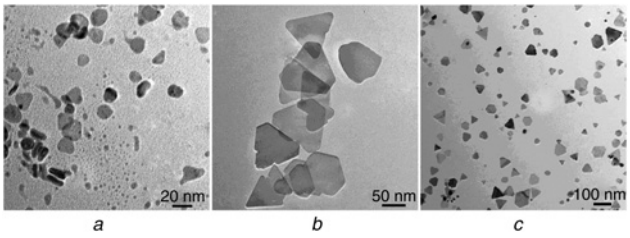

Figure 4 *TEM images of Ag nanostructures synthesised at different PVP concentrations*
a 5 g/l
b 15 g/l
c 20 g/l
SDS, 15 mM; $[Ag(NH_3)_2]^+$, 1 mM; $NaBH_4$, 0.0005 mM

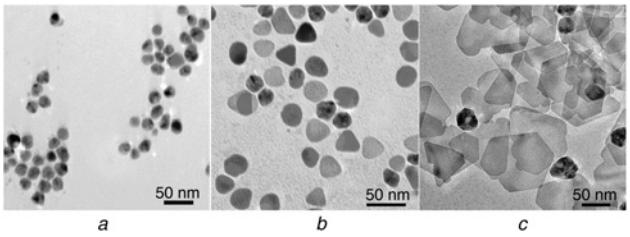

Figure 5 *TEM images of Ag nanostructures synthesised at different SDS concentrations*
a 1 mM
b 8 mM
c 25 mM
PVP, 15 g/l; $[Ag(NH_3)_2]^+$, 1 mM; $NaBH_4$, 0.0005 mM

SDS concentration regulated both the particle size and the morphology, the higher concentrations favoured smaller particle size and nanosheet formation (Fig. 5). In a concentration lower than cac, where both SDS and PVP exist as free monomers, the synthesised nanostructures were Ag nanoparticles of 21 nm in average size (Fig. 5*a*). Then triangular Ag nanosheets with 26, 70 (Fig. 1*b*) and 80–100 nm in edge length became the dominant structures as SDS concentration increased to 8 (Fig. 5*b*), 15 (Fig. 1*b*) and 25 mM (Fig. 5*c*), respectively. This concentration-dependent effect of size was caused by electrostatic attraction between SDS and $[Ag(NH_3)_2]^+$. At higher SDS concentration, more $[Ag(NH_3)_2]^+$ ions can be captured by SDS to the micelles bound to PVP and subsequently reduced by PVP, therefore a more compact structure and bigger size can be formed. In addition, PVP can be selectively absorbed onto the special crystalline facets of Ag nuclei and induce them to grow into different nanostructures [41]. Hence, the formed Ag atoms grew into anisotropic Ag nanosheets by the selective adsorption of PVP onto different crystals.

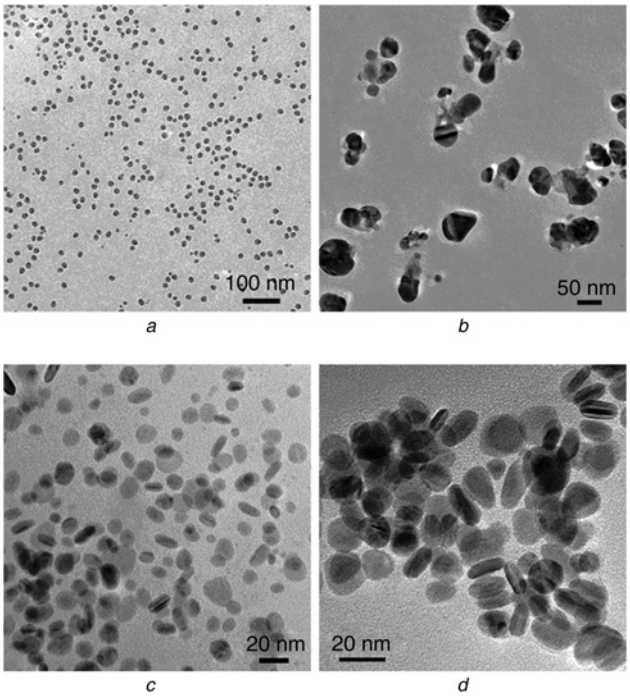

Figure 6 *TEM images of Ag nanostructures obtained at different pH*
a 12.03 pH
b 10.98 pH
c 10.00 pH
d 8.88 pH
PVP, 15 g/l; SDS, 15 mM; $[Ag(NH_3)_2]^+$, 1 mM; $NaBH_4$, 0.0005 mM

doi: 10.1049/mnl.2014.0076

3.4. pH regulation on the morphologies of Ag nanostructures: The pH of reaction solutions can regulate the morphologies of Ag nanostructures by affecting the ionisation state of SDS, $NaBH_4$ and $[Ag(NH_3)_2]^+$. Remarkable variations in the ultimate morphologies of the obtained Ag nanostructures are revealed by Fig. 6. Massive uniform Ag nanoparticles, about 10 nm in diameter, were obtained at pH 12.03 (Fig. 6*a*). Irregular nanoparticles became the dominant products at a pH of 10.98 (Fig. 6*b*); while round Ag nanodiscs with 20 nm diameter were the dominant products with a thickness of 5 nm (Fig. 6*c*) and 10 nm (Fig. 6*d*) which were produced at a pH of 10.00 and 8.88, respectively. Therefore, 2D planar Ag nanostructures trended to generate between a pH of 9 and 10 where the $[Ag(NH_3)_2]^+$ existed at a stable complex ionisation state.

4. Conclusion: Ag nanosheets were synthesised in the microreactor of PVP–SDS aggregations by self-seeding through a facile binary reduction strategy. In this process, Ag nanocrystals were generated firstly from $[Ag(NH_3)_2]^+$ reduced by a trace of $NaBH_4$, and then seeded the subsequent slow growth of anisotropic Ag nanosheets in which PVP served as not only one of the components of the microreactor but also a weak reductant. The experimental results show that concentration variance of the primary reductant $NaBH_4$ induces primary and dramatic differences in both the size and the morphology of the particles. Lower $NaBH_4$ concentration benefits the formation of small and regular nanosheets, while 0.005 mM $NaBH_4$ would induce Ag aggregations. The PVP–SDS aggregations play a very important microreactor role in the fabrication of Ag nanoparticles. When SDS concentrations fall into the PVP–SDS co-assembly concentration range, PVP concentration responds to the particle size, while with SDS concentration below the cac, PVP presents as free monomers and thus it induces irregular particles. The SDS concentration regulates both the particle size and the morphology and there is a concentration dependence on the particle size in the range of 8–25 mM, where the SDS concentration is higher than the cac. The higher SDS concentrations favour smaller particle sizes and nanosheet formation. pH values affect the particle size and the morphology dramatically. 2D planar Ag nanostructures are generated between a pH of 9 and 10, where $[Ag(NH_3)_2]^+$ exists at a stable complex ionisation state.

5. Acknowledgments: The authors acknowledge support from the National Natural Science Foundation of China (nos 21276113 and 20871059).

6 References

[1] Chen Z., Zhang G., Chen X., Chen J., Liu J., Yuan H.: 'A fluorescence switch sensor for 6-mercaptopurine detection based on gold nanoparticles stabilized by biomacromolecule', *Biosens. Bioelectron.*, 2013, **41**, pp. 844–847

[2] Yahyaei B., Azizian S.: 'Rapid photogeneration of silver nanoparticles in ethanolic solution: a kinetic study', *Spectrochim. Acta A*, 2013, **101**, pp. 343–348

[3] Vodnik V.V., Šaponjić Z., Džunuzović J.V., Bogdanović U., Mitrić M., Nedeljković J.: 'Anisotropic silver nanoparticles as filler for the formation of hybrid nanocomposites', *Mater. Res. Bull.*, 2013, **48**, (1), pp. 52–57

[4] Tijing L.D., Amarjargal A., Jiang Z., *ET AL.*: 'Antibacterial tourmaline nanoparticles/polyurethane hybrid mat decorated with silver nanoparticles prepared by electrospinning and UV photoreduction', *Curr. Appl. Phys.*, 2013, **13**, (1), pp. 205–210

[5] Gu S., Wang W., Wang H., Tan F., Qiao X., Chen J.: 'Effect of aqueous ammonia addition on the morphology and size of silver particles reduced by ascorbic acid', *Powder Technol.*, 2013, **233**, pp. 91–95

[6] Esmaeili M., Madaeni S.S., Barzin J.: 'The effect of carrier salts blending on the morphology, stability and permeation properties of PES/PEO facilitated transport membranes', *Sep. Purif. Technol.*, 2013, **103**, pp. 289–305

[7] Chen T.Y., Chiu C.K., Choi Y.J., Luo T.J.M., Lin T.L.: 'Formation of self-aggregated and interconnected silver network within sol-gel silica', *J. Mater. Sci.*, 2013, **48**, (2), pp. 850–856

[8] Zhu G., Chen D.: 'Solvothermal fabrication of uniform silver nanowires', *J. Mater. Sci., Mater. Electron.*, 2012, **23**, (11), pp. 2035–2041

[9] Zhou M., Xia G., Chai L., Li J., Zhou L.: 'Analysis of flow and heat transfer characteristics of micro-pin fin heat sink using silver nanofluids', *Sci. Chin. Technol. Sc.*, 2012, **55**, (1), pp. 155–162

[10] Zhou Y., Zhao Y., Wang L., Xu L., Zhai M., Wei S.: 'Radiation synthesis and characterization of nanosilver/gelatin/carboxymethyl chitosan hydrogel', *Radiat. Phys. Chem.*, 2012, **81**, (5), pp. 553–560

[11] Chen H., Liu Y., Zhao G.: 'Synthesis and characterization of hollow silver spheres at room temperature', *Electron. Mater. Lett.*, 2011, **7**, (2), pp. 151–154

[12] Aksomaityte G., Poliakoff M., Lester E.: 'The production and formulation of silver nanoparticles using continuous hydrothermal synthesis', *Chem. Eng. Sci.*, 2013, **85**, pp. 2–10

[13] Yan J., Zou G., Wu A., *ET AL.*: 'Effect of PVP on the low temperature bonding process using polyol prepared Ag nanoparticle paste for electronic packaging application', *J. Phys., Conf. Ser.*, 2012, **379**, (1), pp. 012024/1–012024/6

[14] Hebeish A., Hashem M., El-Hady M.M.A., Sharaf S.: 'Development of CMC hydrogels loaded with silver nano-particles for medical applications', *Carbohyd. Polym.*, 2013, **92**, (1), pp. 407–413

[15] Darmanin T., Nativo P., Gilliland D., *ET AL.*: 'Microwave-assisted synthesis of silver nanoprisms/nanoplates using a modified polyol process', *Colloids Surf. A*, 2012, **395**, pp. 145–151

[16] Lin C.H., Chen W.L., Du C.H., Wan C.C., Wang Y.Y.: 'Fabrication of metal grid on silicon-based solar cell by electrochemical deposition and microcontact print'. 35th IEEE Photovoltaic Specialists Conf. (PVSC), Honolulu, Hawaii, 2010, pp. 001330–001334

[17] Pedroza-Toscano M.A., Rabelero-Velasco M., Diaz de Leon R., *ET AL.*: 'Preparation of silver nanostructures from bicontinuous microemulsions', *J. Nanomater.*, 2012, **2012**, pp. 1–7

[18] Safin D.A., Mdluli P.S., Revaprasadu N., *ET AL.*: 'Nanoparticles and thin films of silver from complexes of derivatives of N-(diisopropylthiophosphoryl) thioureas', *Chem. Mater.*, 2009, **21**, (18), pp. 4233–4240

[19] Luu Q.N., Doorn J.M., Berry M.T., Jiang C., Lin C., May P.S.: 'Preparation and optical properties of silver nanowires and silver-nanowire thin films', *J. Colloid Interface Sci.*, 2011, **356**, (1), pp. 151–158

[20] Sarkar P., Bhui D.K., Bar H., *ET AL.*: 'DDA-based simulation of UV-Vis extinction spectra of Ag nanorods synthesized through seed-mediated growth process', *Plasmonics*, 2011, **6**, (1), pp. 43–51

[21] Jiang X., Yu A.: 'Low dimensional silver nanostructures: synthesis, growth mechanism, properties and applications', *J. Nanosci. Nanotechnol.*, 2010, **10**, (12), pp. 7829–7875

[22] He X., Zhao X.: 'Solvothermal synthesis and formation mechanism of chain-like triangular silver nanoplate assemblies: application to metal-enhanced fluorescence (MEF)', *Appl. Surf. Sci.*, 2009, **255**, (16), pp. 7361–7368

[23] Liu L., Wei T., Guan X., Zi X., He H., Dai H.: 'Size and morphology adjustment of PVP-stabilized silver and gold nanocrystals synthesized by hydrodynamic assisted self-assembly', *J. Phys. Chem. C*, 2009, **113**, (20), pp. 8595–8600

[24] Jiang L.P., Xu S., Zhu J.M., Zhang J.R., Zhu J.J., Chen H.Y.: 'Ultrasonic-assisted synthesis of monodisperse single-crystalline silver nanoplates and gold nanorings', *Inorg. Chem.*, 2004, **43**, (19), pp. 5877–5883

[25] Sarkar P., Bhui D.K., Bar H., *ET AL.*: 'Aqueous-phase synthesis of silver nanodiscs and nanorods in methyl cellulose matrix: photophysical study and simulation of UV-vis extinction spectra using DDA method', *Nanoscale Res. Lett.*, 2010, **5**, (10), pp. 1611–1618

[26] Zhang L., Chai L., Duan J., *ET AL.*: 'One-step and cost-effective synthesis of micrometer-sized saw-like silver nanosheets by oil/water interfacial method', *Mater. Lett.*, 2011, **65**, (9), pp. 1295–1298

[27] Du S., Kendall K., Toloueinia P., Mehrabadi Y., Gupta G., Newton J.: 'Aggregation and adhesion of gold nanoparticles in phosphate buffered saline', *J. Nanoparticles. Res.*, 2012, **14**, (3), pp. 758/1–758/14

[28] Zhu W., Romanski F.S., Dalvi S.V., Dave R.N., Silvina Tomassone M.: 'Atomistic simulations of aqueous griseofulvin crystals in the presence of individual and multiple additives', *Chem. Eng. Sci.*, 2012, **73**, pp. 218–230

[29] Ren Y., Xu C., Wu M., Niu M., Fang Y.: 'Controlled synthesis of gold nanoflowers assisted by poly(vinyl pyrrolidone)-sodium dodecyl sulfate aggregations', *Colloids Surf. A*, 2011, **380**, (1–3), pp. 222–228

[30] Zhu W., Romanski F.S., Meng X., Mitra S., Tomassone M.S.: 'Atomistic simulation study of surfactant and polymer interactions on the surface of a fenofibrate crystal', *Eur. J. Pharm. Sci.*, 2011, **42**, (5), pp. 452–461
[31] Fang Y., Ren Y., Jiang M.: 'Co-effect of soft template and microwave irradiation on morphological control of gold nanobranches', *Colloid Polym. Sci.*, 2011, **289**, (15–16), pp. 1769–1776
[32] Jin R., Cao Y., Mirkin C.A., Kelly K.L., Schatz G.C., Zheng J.G.: 'Photoinduced conversion of silver nanospheres to nanoprisms', *Science*, 2001, **294**, (5548), pp. 1901–1903
[33] Taylor D.J.F., Thomas R.K., Penfold J.: 'Polymer/surfactant interactions at the air/water interface', *Adv. Colloid Interface Sci.*, 2007, **132**, (2), pp. 69–110
[34] Shen Q., Wei H., Wang L., *ET AL.*: 'Crystallization and aggregation behaviors of calcium carbonate in the presence of poly(vinyl pyrrolidone) and sodium dodecyl sulfate', *J. Phys. Chem. B*, 2005, **109**, (39), pp. 18342–18347
[35] Fan Y., Fang Y.: 'Controlled synthesis of hollow Cu_2O submicrospheres by SDS-PVP necklace-like soft clusters and their optical properties'. AIChE Annual Meeting, Conf. Proc., Salt Lake City, UT, USA, November 2010, pp. a71/1–a71/5
[36] Wang C.R., Fang Y., Li B.: 'Self-assembly of multipod-like gold nanoparticles in the soft template of SDS-PVP clusters', *Acta Phys., Chim. Sin.*, 2008, **24**, (1), pp. 183–186
[37] Fan Y., Fang Y., Gou Y., Ke L.: 'Synthesis of hollow Cu_2O submicrospheres by SDS-PVP necklace-like soft clusters'. AIChE Annual Meeting, Conf. Proc., Nashville, TN, USA, November 2009, pp. fan13/1–fan13/6
[38] Fang Y., Xia Y., Cai K., Liu X., Zong L., Ma L.: 'Critical concentration of surfactant in clusterization of $ROSO_3Na$ homologs on nonelectrolytic macromolecules', *Acta Polym. Sin.*, 2003, **1**, (4), pp. 530–534
[39] Xia Y., Xiong Y., Lim B., Skrabalak S.E.: 'Shape-controlled synthesis of metal nanocrystals: simple chemistry meets complex physics?', *Angew. Chem. Int. Ed.*, 2009, **48**, (1), pp. 60–103
[40] Xia X., Zeng J., Zhang Q., Moran C.H., Xia Y.: 'Recent developments in shape-controlled synthesis of silver nanocrystals', *J. Phys. Chem. C*, 2012, **116**, (41), pp. 21647–21656
[41] Xia X., Zeng J., Oetjen L.K., Li Q., Xia Y.: 'Quantitative analysis of the role played by poly(vinyl pyrrolidone) in seed-mediated growth of Ag nanocrystals', *J. Am. Chem. Soc.*, 2012, **134**, (3), pp. 1793–1801

doi: 10.1049/mnl.2014.0076